Volume 5
Number 16
21 August 2024
Pages 6335–6674

Materials Advances

rsc.li/materials-advances

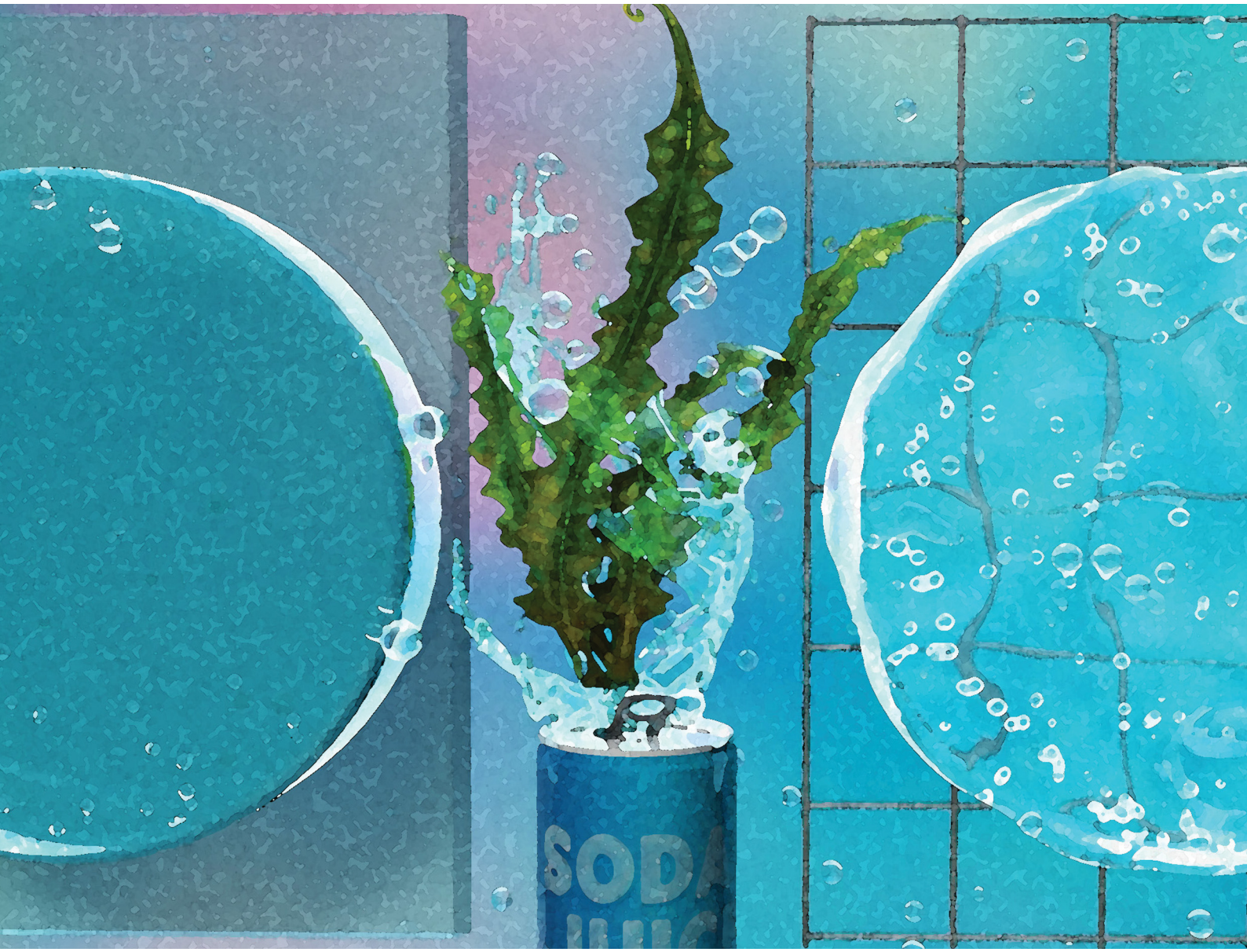

ISSN 2633-5409

ROYAL SOCIETY OF CHEMISTRY

COMMUNICATION

Ryota Teshima *et al.*

Effect of CO_2 release behavior on the crosslinking degree of alginate hydrogels prepared with $CaCO_3$ and carbonated water

Materials Advances

ROYAL SOCIETY OF CHEMISTRY

COMMUNICATION

View Article Online
View Journal | View Issue

Check for updates

Cite this: *Mater. Adv.*, 2024, 5, 6368

Received 13th March 2024,
Accepted 2nd June 2024

DOI: 10.1039/d4ma00257a

rsc.li/materials-advances

Effect of CO_2 release behavior on the crosslinking degree of alginate hydrogels prepared with $CaCO_3$ and carbonated water†

Ryota Teshima, *[a] Shigehito Osawa, ‡[bc] Kaoru Hirose, [d] Yayoi Kawano, §[d] Akihiko Kikuchi, [e] Takehisa Hanawa [d] and Hidenori Otsuka [abc]

Carbonated water facilitates the gelation of alginate and $CaCO_3$ solutions. The rapid release of CO_2 from the hydrogels after gelation resulted in a faster pH increase, lower amount of $CaCO_3$ dissolution, and lower crosslinking degree. The CO_2 release behavior, *i.e.*, "post-gelation condition," affects the degree of crosslinking, an essential parameter for determining hydrogel properties.

Hydrogels—soft materials containing water molecules in a three-dimensional network structure of crosslinked polymers—are widely applied in life sciences.[1–3] In particular, hydrogels composed of biopolymers such as polysaccharides[4,5] and proteins[6,7] have attracted attention owing to their safety, biocompatibility, and ability to form supramolecular assemblies. These biopolymers can be physically crosslinked by changing the solution environment, such as the pH.[8,9] Hydrogels based on physical crosslinking have been widely studied for biomedical applications. However, when the pH of the entire solution is reduced by adding acidic agents, the acidic agents often remain in the hydrogel and cause acidification, which can harm living organisms.[10]

Recently, a new gelation system introducing carbon dioxide (CO_2) gas into biopolymer solutions has attracted attention.[11–18] In this gelation method, CO_2 functions as an acidic agent that reduces the system's pH and is released into the atmosphere after gelation, preventing acidification of the hydrogel. Floren *et al.* successfully gelled silk fibroin without acidification by introducing high-pressure CO_2.[15] In commonly used methods, polysaccharides such as alginate or pectin are crosslinked with Ca^{2+} *via* physical interactions with the carboxy groups of the polymer using $CaCO_3$ as a Ca^{2+} source;[11–13] Gurikov *et al.* demonstrated high-pressure CO_2 into a mixture of alginate and $CaCO_3$ to reduce the pH of the solution and produce Ca^{2+} from $CaCO_3$ for forming an alginate hydrogel.[11] Hydrogels prepared with high-pressure CO_2 have a controlled porous structure composed of CO_2 that can be applied as an effective cell scaffold[16,17] because it aids in nutrient penetration and cell migration. In addition, this gelation method can be hybridized with other biopolymers, such as lignin[16] and carrageenan,[18] to achieve enhanced functionality. The effects of CO_2 introduction and release conditions on hydrogel properties have been studied to broaden the hydrogel application scope but are not fully understood. In particular, the effect of the CO_2 release behavior after gelation, that is, the post-gelation conditions, is unclear because of the preconceived notion that the hydrogel properties are controlled by pre-gelation conditions, such as polymer and crosslinker concentrations. Martins *et al.* examined the effect of the CO_2 depressurization rate on the hydrogel structure, revealing that faster depressurization corresponded to a higher degree of CO_2 gas expansion and complicated the comparison of hydrogel physicochemical properties, such as the crosslinking degree.[17] In addition, the effects of the depressurization rate on the mechanical structure of hydrogels remain debatable,[16,17] as pressure changes complicate the physicochemical comparison of the hydrogel structures. An understanding of the effects of CO_2 release conditions on hydrogel properties, especially the

[a] *Department of Chemistry, Graduate School of Science, Tokyo University of Science, 1-3 Kagurazaka, Shinjuku, Tokyo 162-8601, Japan. E-mail: 1322595@ed.tus.ac.jp*
[b] *Department of Applied Chemistry, Faculty of Science, Tokyo University of Science, 1-3 Kagurazaka, Shinjuku, Tokyo 162-8601, Japan*
[c] *Water Frontier Research Center (WaTUS), Research Institute for Science and Technology, Tokyo University of Science, 1-3 Kagurazaka, Shinjuku, Tokyo 162-8601, Japan*
[d] *Department of Pharmacy, Faculty of Pharmaceutical Sciences, Tokyo University of Science, 2641 Yamazaki, Noda, Chiba 278-8510, Japan*
[e] *Department of Materials Science and Technology, Faculty of Advanced Engineering, Tokyo University of Science, 6-3-1 Niijuku, Katsushika, Tokyo 125-8585, Japan*

† Electronic supplementary information (ESI) available: Experimental section, molar concentration of alginate and $CaCO_3$, SEM and phase-contrast image of Alg-gel, definition of Alg-gel surfaces, thickness changes of Alg-gel and stress–strain curves of Alg-gel. See DOI: https://doi.org/10.1039/d4ma00257a

‡ Current affiliation: Department of Biomedical Engineering, Faculty of Life Sciences, Toyo University, 48-1 Oka, Asaka, Saitama 351-8510, Japan.
§ Current affiliation: Department of Clinical Pharmacy, Graduate School of Pharmaceutical Sciences, Nagoya City University, 3-1 Tanabe-dori, Mizuho, Nagoya 467-8603, Japan.

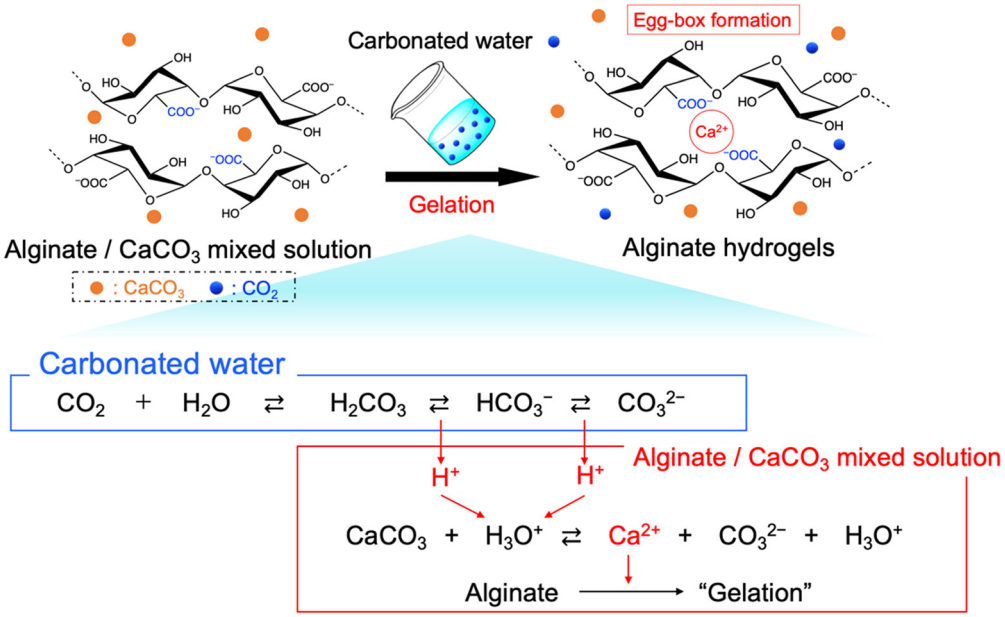

Fig. 1 The gelation mechanism of alginate hydrogels prepared with $CaCO_3$ and carbonated water.

crosslinking degree, would greatly expand the hydrogel application scope from the materials field to the medical field, because the crosslinking degree affects both the physicochemical (*e.g.*, mechanical strength and swelling ratio) and biological (*e.g.*, cell migration) properties of hydrogels.

In this study, we prepared the alginate hydrogels (Alg-gel) with $CaCO_3$ and carbonated water and investigated the effect of CO_2 release from the hydrogels on the degree of crosslinking. The gelation mechanism of the alginate with $CaCO_3$ and carbonated water is shown in Fig. 1. In previously reported gelation methods using high-pressure CO_2,[11–18] precise control of the CO_2 pressure was essential for controlling the physicochemical properties of hydrogels, but this makes comparison of hydrogel properties difficult. In contrast, our method enabled facile hydrogel synthesis under ambient conditions and, hence, the comparison of the physicochemical properties of the hydrogels without the effect of CO_2 gas expansion. As previously reported,[19–21] Alg-gels were prepared with carbonated water. The relationship between the concentration of calcium-binding units in alginate (concentration of carboxy groups in guluronic acid) and $CaCO_3$ is shown in Table S1 (ESI†). When carbonated water with the pH of 3.64 ± 0.06 (n = 3, mean ± standard deviation)[20] was added to the alginate/$CaCO_3$ mixed solution, an Alg-gel was obtained within 4 min (Fig. S1a, ESI†). A scanning electron microscopy (SEM) image of the cross-section of the Alg-gel showed a porous structure, indicating that the alginate was crosslinked by Ca^{2+} (Fig. S1b, ESI†). Furthermore, the phase-contrast image of the Alg-gel revealed

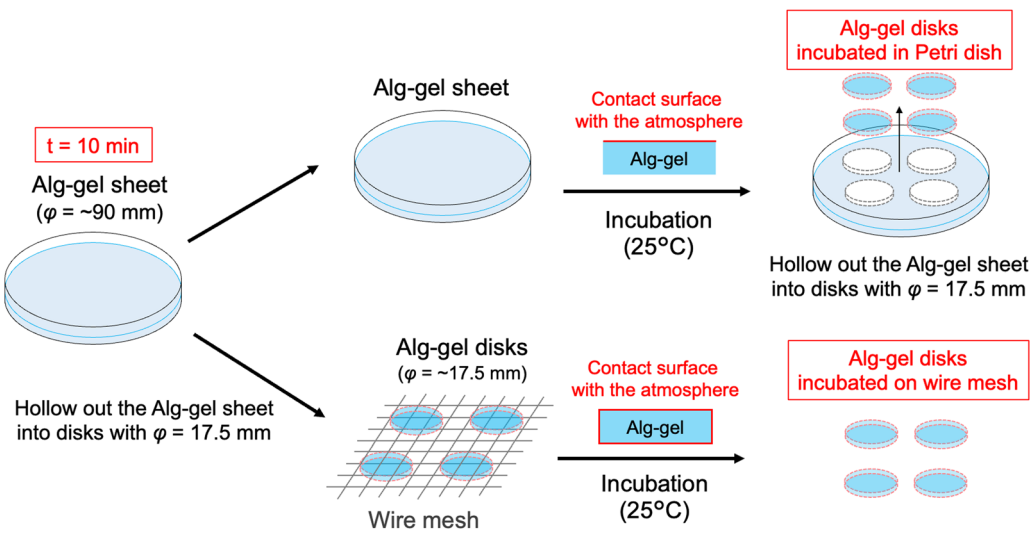

Fig. 2 Schematic of Alg-gel disks incubated in a Petri dish and on a wire mesh. t = 0 refers to the time as carbonated water was added.

the $CaCO_3$ crystals in the hydrogel (Fig. S1c, ESI†). To control the release of CO_2 from the Alg-gel and $CaCO_3$ dissolution, we adjusted the contact area between the Alg-gel surface and the atmosphere. Specifically, we prepared two types of Alg-gels with different air contact areas (Fig. 2). First, Alg-gel sheet was prepared and incubated in Petri dish such that only the top surface of the gel was in contact with the atmosphere. The Alg-gel sheet was cut into 17.5-mm disks for evaluation. Second, Alg-gel sheet was prepared in the same manner, hollowed out into a 17.5-mm disk 10 min after preparation, and incubated on a wire mesh so that the entire surface of the gel was in contact with the atmosphere.

To visually capture the release behavior of CO_2 from the Alg-gel, the Alg-gel was stained with bromothymol blue (BTB) as a pH indicator, which appeared yellow, green, and blue under acidic, neutral, and alkaline conditions, respectively (Fig. 3). The Alg-gel disk incubated in the Petri dish changed slightly to neutral over 60 min, indicating that CO_2 was released slowly into the atmosphere. However, the Alg-gel disk incubated on the wire mesh became alkaline at t = 20 min, and the entire gel disk became alkaline at t = 40 min. These results indicated that the CO_2 in the Alg-gel disk incubated on the wire mesh was released quickly into the atmosphere because all the surfaces of the gel were in contact with the atmosphere. Thereafter, the Alg-gel disk incubated in the Petri dish turned completely blue. Interestingly, the color change of the Alg-gel disk incubated on the wire mesh began around the gel disk. Details regarding the behavior of CO_2 release from each surface would be interesting to investigate in the future.

To quantitatively evaluate the pH change behavior shown in Fig. 3, the surface pH values of the Alg-gels in the Petri dish and on the wire mesh were measured over 300 min (Fig. 4). The difference in surface pH between the Alg-gel surface exposed to the atmosphere—denoted as the front surface—and that in contact with the bottom of the dish—denoted as the back surface—was examined (Fig. S2, ESI†). Unfortunately, the pH of the side surface of the Alg-gel disk could not be measured, because the side surface area was too small. The surface pH values of the Alg-gel disks incubated in a Petri dish are shown in Fig. 4a. The pH of the front surface increased faster than that of the back surface. The release of CO_2 from the Alg-gel disk incubated in the Petri dish delayed the pH change on the back surfaces. Notably, no pH gradient appeared in the mixture of $CaCO_3$ and carbonated water without alginate, implying that carbonate ions and CO_2 exhibited different behaviors in the hydrogels.[20] At t = 300 min, the pH values of the front and back surfaces were almost equal (8.5), indicating that all the CO_2 in the Alg-gel disk was released. In contrast, different release behavior of CO_2 was observed for the Alg-gel disks incubated on wire mesh (Fig. 4b). At t = 10 min, the pH of the Alg-gel disks was higher on the front surface than on the back surface because the gel disks were incubated in Petri dishes. However, at t = 30 min, the pH values of the front and back surfaces were identical. Thus, the Alg-gel disks incubated on the wire mesh immediately exhibited no delay in pH change because the front and back surfaces of the gel disk were in contact with the atmosphere. At t = 90 min, the pH values of the front and back surfaces converged to 8.5, as indicated by the BTB color change shown in Fig. 3. In addition, the pH of the front surface of the Alg-gel disks incubated on the wire mesh increased faster than those of the disks incubated in the Petri dish. This may be due to the release of CO_2 from the entire surface of Alg-gel disks incubated on the wire mesh, as shown in Fig. 3. These results suggest that the Alg-gel disks on the wire mesh released CO_2 faster into the atmosphere than those in the Petri dish.

The incubation method of the Alg-gel disks influences the release behavior of CO_2 from the gel disks, which motivated us to compare the degrees of crosslinking. The rapid release of CO_2 from the hydrogels after gelation may result in lower amount of $CaCO_3$ dissolution, and lower crosslinking degree. As shown in Fig. 3 and 4, for the Alg-gel disks incubated on the wire mesh, CO_2 release was complete after only 90 min. Therefore, the disks were incubated on the wire mesh for 90 min to achieve complete CO_2 release and then transferred to the Petri dish to prevent moisture loss. The procedure used to prepare the Alg-gel disks for mechanical evaluations is shown in Fig. 5. As shown in Fig. S3 (ESI†), the thicknesses of the disks incubated in the Petri dish and on the wire mesh were almost the same. After adjusting the conditions, Young's moduli of the Alg-gel disks were measured *via* a compression test (Fig. 6a). The Young's modulus was calculated from the slope of 3% compressive strain, and the Young's modulus of Alg-gel disks incubated in the Petri dish were significantly higher than those of Alg-gel disks incubated on the wire mesh.

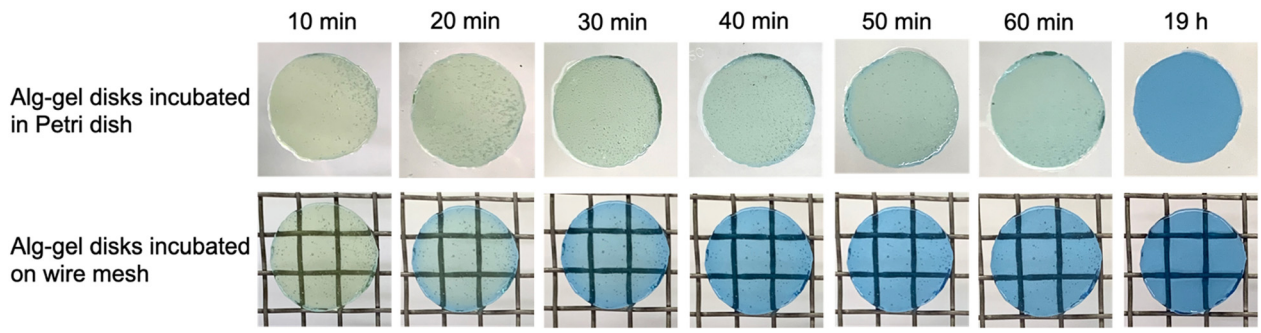

Fig. 3 pH changes of Alg-gel disks incubated in a Petri dish and on a wire mesh containing BTB over time (t = 0 refers to the time when carbonated water was added). The diameter of Alg-gel disks was ~17.5 mm, and the thickness was 3.46 ± 0.26 mm.

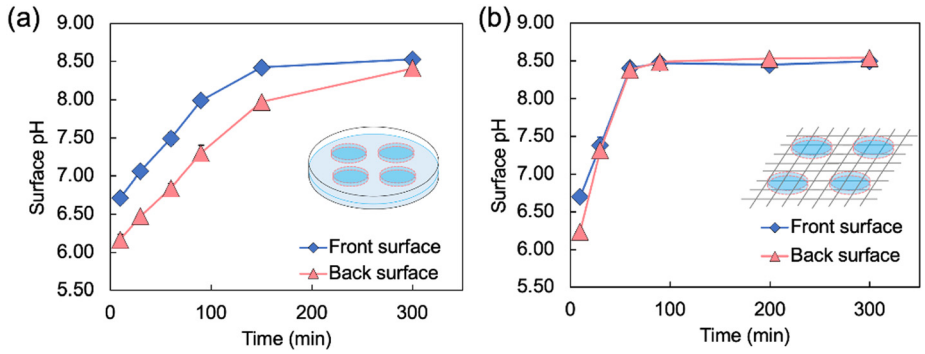

Fig. 4 Changes in the surface pH of Alg-gel disks incubated (a) in a Petri dish* and (b) on a wire mesh over time (t = 0 refers to the time when carbonated water was added). The thickness of the Alg-gel disks was 3.46 ± 0.26 mm. Values are expressed as the mean ± SE obtained from n = 3–4. * This result has been reproduced from previous our study.[19]

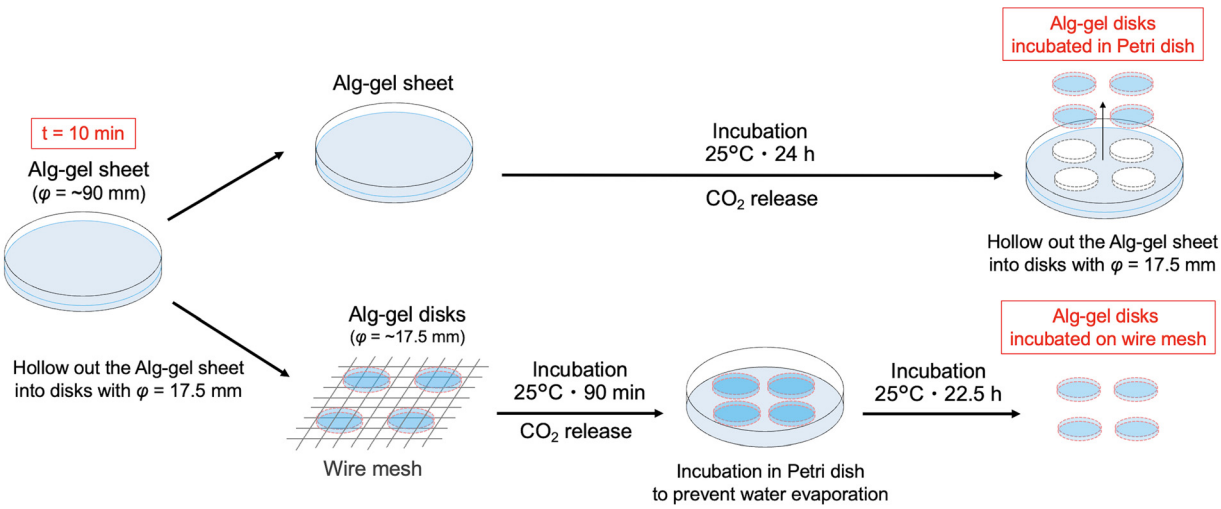

Fig. 5 Schematic preparation of the Alg-gel disks incubated in the Petri dish and on the wire mesh for mechanical evaluations. t = 0 refers to the time as carbonated water was added.

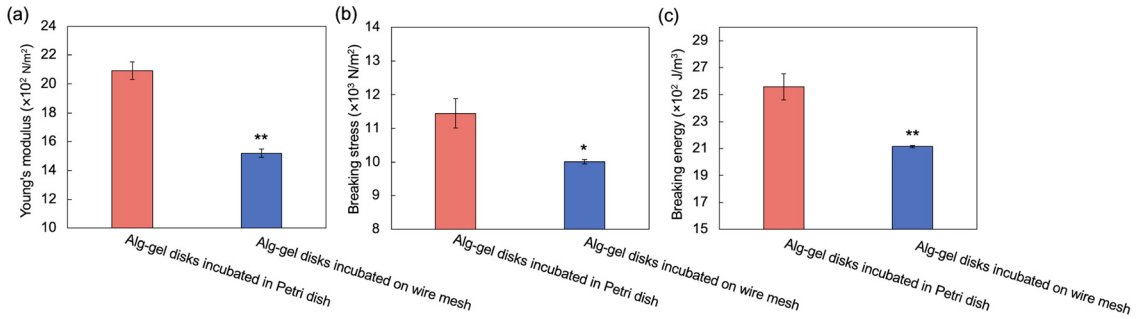

Fig. 6 The mechanical properties of Alg-gel disks incubated in a Petri dish and on a wire mesh. (a) Young's modulus of Alg-gel disks incubated in a Petri dish and on a wire mesh. Values are expressed as the mean ± SE obtained from n = 6. (b) Breaking stress of Alg-gel disks incubated in a Petri dish and on a wire mesh. (c) Breaking energy of Alg-gel disks incubated in a Petri dish and on a wire mesh. Values are expressed as the mean ± SE obtained from n = 3–4. *p < 0.05, **p < 0.01 *versus* Alg-gel disks in a Petri dish.

Furthermore, we investigated the mechanical properties of the Alg-gel disks incubated in a Petri dish and wire mesh. The Alg-gel disks were compressed to 87% strain, and the breaking stress and energy were calculated. All the stress–strain curves are shown in Fig. S4 (ESI†). The breaking stress of the Alg-gel disks incubated in the Petri dish was significantly higher than

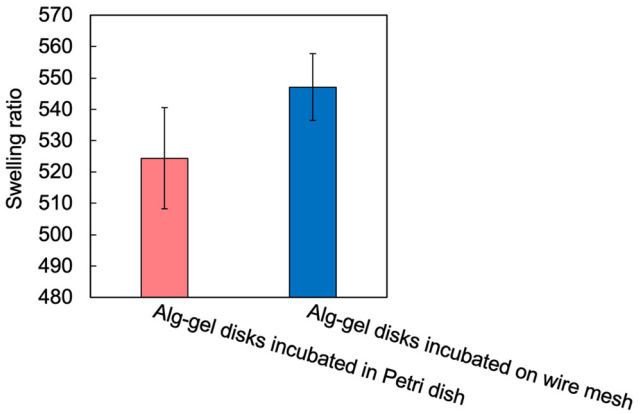

Fig. 7 Swelling ratio of Alg-gel disks in a Petri dish and on a wire mesh. Values are expressed as the mean ± SE obtained from n = 5–6.

that of the disks incubated on the wire mesh (Fig. 6b). Additionally, the breaking energy of the disks incubated in the Petri dish was significantly higher than that of the disks incubated on the wire mesh (Fig. 6c). These results indicate that the degree of crosslinking differed between the Alg-gel disks incubated in the Petri dish and on the wire mesh and that the behavior of CO_2 release from the Alg-gel affected the degree of crosslinking. Additionally, the Alg-gel disk incubated on the wire mesh had a higher swelling ratio than that incubated in the Petri dish (Fig. 7). These results indicate that the degree of crosslinking of the Alg-gel disks incubated on the wire mesh was lower than that of the Alg-gel disks incubated in the Petri dish. Therefore, the rapid release of CO_2 from the hydrogels after gelation resulted in faster pH increase, lower amount of $CaCO_3$ dissolution, and lower crosslinking degree.

In general, the degree of hydrogel crosslinking is an important parameter governing physicochemical properties, such as the swelling ratio and mechanical strength, and biological properties, such as the migration of encapsulated cells. The degree of crosslinking of hydrogels tends to be controlled by ''pre-gelation parameters'' such as the polymer and crosslinker concentrations. However, the crosslinking degree of the hydrogels prepared with CO_2 as the acidic agent and $CaCO_3$ as the crosslinking agent source was affected by post-gelation conditions, namely the contact area between the hydrogel and the atmosphere after gelation. The rapid release of CO_2 from the hydrogels after gelation lowered the system's pH and reduced the crosslinking degree. In future studies, the polymer network structure and potential applications of these hydrogels as functional materials should be examined in detail. Especially, the molecular weight of alginate may affect these properties and applications. In addition, elucidating the mass balance and kinetics of the gelation reaction may contribute to the control of gelation reactions.

Conflicts of interest

There are no conflicts to declare.

Acknowledgements

The authors thank Kimica Corp. (Tokyo, Japan) for providing alginates. This work was supported by Grants-in-Aid for Research Activities from the Masason Foundation [grant numbers: GD14469, GD9675, and GD2825] and Grants-in-Aid for Extracurricular Activities for Students at Tokyo University of Science Parents Associations (Kouyoukai) [grant number: 2019-15].

References

1 X. Liu, S. Zhou, B. Cai, Y. Wang, D. Deng and X. Wang, *Biomater. Sci.*, 2022, **10**, 3480.
2 S. H. Jeong, M. Kim, T. Y. Kim, H. Kim, J. H. Ju and S. K. Hahn, *ACS Appl. Bio Mater.*, 2020, **3**, 5040.
3 H. Mamada, A. Kemmochi, T. Tamura, Y. Shimizu, Y. Owada, Y. Ozawa, K. Hisakura, T. Oda, N. Ohkohchi, Y. Kawano and T. Hanawa, *Polym. Adv. Technol.*, 2022, **33**, 125.
4 C. J. Maxwell, A. M. Soltisz, W. W. Rich, A. Choi, M. A. Reilly and K. E. Swindle-Reilly, *J. Biomed. Mater. Res. A*, 2022, **110**, 1621.
5 F. Marin, M. C. Tanzi and P. Petrini, *Int. J. Biol. Macromol.*, 2012, **51**, 681.
6 Ł. Mazurek, M. Szudzik, M. Rybka and M. Konop, *Biomolecules*, 2022, **12**, 1852.
7 S. Indrakumar, A. Joshi, T. K. Dash, V. Mishra, B. Tandon and K. Chatterjee, *Int. J. Biol. Macromol.*, 2023, **233**, 123569.
8 A. E. Terry, D. P. Knight, D. Porter and F. Vollrath, *Biomacromolecules*, 2004, **5**, 768.
9 K. Y. Lee and D. J. Mooney, *Prog. Polym.*, 2012, **37**, 106.
10 H. R. Moreira, F. Munarin, R. Gentilini, L. Visai, P. L. Granja, M. C. Tanzi and P. Petrini, *Carbohydr. Polym.*, 2014, **103**, 339.
11 P. Gurikov, S. P. Raman, D. Weinrich, M. Fricke and I. Smirnova, *RSC Adv.*, 2015, **5**, 7812.
12 I. Preibisch, L. M. Ränger, P. Gurikov and I. Smirnova, *Gels*, 2020, **6**, 28.
13 P. Gurikov and I. Smirnova, *Gels*, 2018, **4**, 14.
14 S. Napavichayanun, W. Bonani, Y. Yang, A. Motta and P. Aramwit, *Adv. Wound Care*, 2019, **8**, 452.
15 M. L. Floren, S. Spilimbergo, A. Motta and C. Migliaresi, *Biomacromolecules*, 2012, **13**, 2060.
16 S. Quraishi, M. Martins, A. A. Barros, P. Gurikov, S. P. Raman, I. Smirnova, A. R. C. Duarte and R. L. Reis, *J. Supercrit. Fluids*, 2015, **105**, 1.
17 M. Martins, A. A. Barros, S. Quraishi, P. Gurikov, S. P. Raman, I. Smirnova, A. R. C. Duarte and R. L. Reis, *J. Supercrit. Fluids*, 2015, **106**, 152.
18 M. Alnaief, B. Mohammad, M. Aljarrah and R. M. Obaidat, *Jordan J. Phys.*, 2019, **12**, 79.
19 R. Teshima, S. Osawa, M. Yoshikawa, Y. Kawano, H. Otsuka and T. Hanawa, *Int. J. Biol. Macromol.*, 2024, **254**, 127928.
20 R. Teshima, S. Osawa, Y. Kawano, T. Hanawa, A. Kikuchi and H. Otsuka, *ACS Omega*, 2023, **8**, 7800.
21 R. Teshima, Y. Kawano, T. Hanawa and A. Kikuchi, *Polym. Adv. Technol.*, 2020, **31**, 3032.